Mesoporous silica nanoparticle-based protein delivery systems for biomedical applications

Tu, J.

Chapter V

Lipid Bilayer-Coated Mesoporous Silica Nanoparticles Carrying Bovine Hemoglobin as an Erythrocyte Mimic

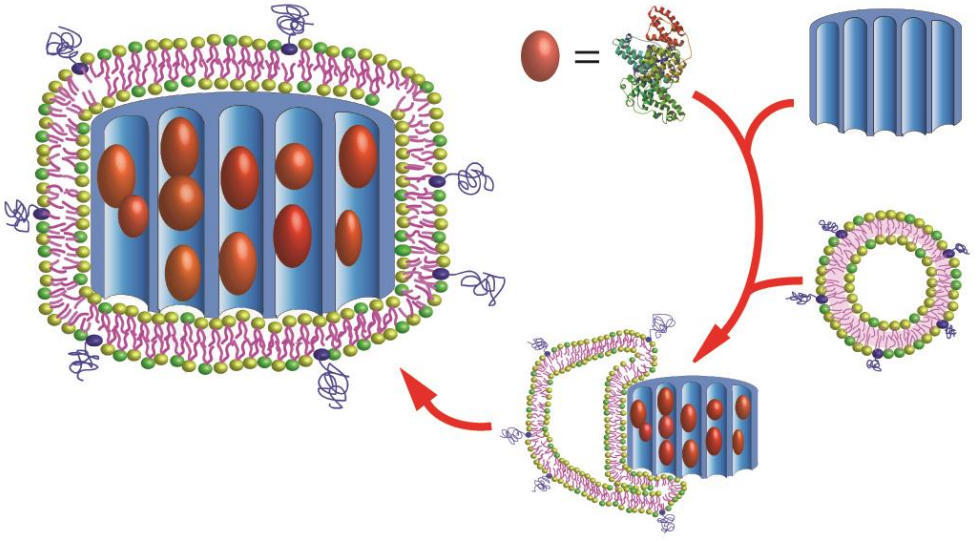

Jing Tu, Jeroen Bussmann, Guangsheng Du, Yue Gao, Joke A. Bouwstra, Alexander Kros

Abstract

Hemoglobin (Hb)-loaded mesoporous silica nanoparticles (MSNs) coated with a lipid bilayer (LB-MSNs) were investigated as an erythrocyte mimic. MSNs with a large average pore size (10 nm) act as a rigid core and provide a protective environment for Hb encapsulated inside the pores. The colloidal stability of Hb-loaded MSNs was enhanced upon the application of a lipid bilayer, through fusion of PEGylated liposomes onto the exterior surface of Hb-loaded MSNs. The morphology and mesostructure of the MSNs were characterized by scanning electron microscopy (SEM), transmission electron microscopy (TEM) and surface area analysis. The Hb loading capacity (LC%) in MSNs was studied by thermogravimetric analysis (TGA). UV-Visible absorption spectroscopy revealed that Hb inside MSNs had an identical, but slightly broadened peak in the Soret region compared to free Hb. Furthermore the encapsulated Hb exhibits similar peroxidase-like activity in catalyzing the oxidation of 2,2′-azino-bis(3-ethylbenzothiazoline-6-sulfonic acid) diammonium salt (ABTS) with hydrogen peroxide. The introduction of a supported lipid bilayer (LB) demonstrated the potential to prevent premature Hb release and increased the colloidal stability of the Hb-loaded MSNs. The *in vivo* systemic circulation and biodistribution of LB-MSNs were studied in optically transparent zebrafish embryos, revealing that LB-MSNs have the potential to act as an erythrocyte mimic.

Keywords: mesoporous silica nanoparticles, hemoglobin, lipid bilayer, zebrafish embryos, erythrocyte mimic

5.1 Introduction

Due to the shortage of blood donations and the risks associated with allogenic donor blood transfusion, such as virus infection, and unmatched blood types, artificial red blood cell (RBC) substitutes have been investigated intensively during the past decades.[1-3] To mimic and fulfil some functions of RBCs, there are two main types of artificial RBC substitute in development.[2, 4] Apart from perfluorocarbon emulsion-based substitutes,[5] hemoglobin (Hb, 6.5 × 5.4 × 5.5 nm, Mw 64500)-based oxygen carriers (HBOC) have attracted increasing attention.[6] Hb is the essential oxygen carrying protein in erythrocytes.[7] Pioneering work was performed with stroma-free Hb,[2, 8-11] which unfortunately was unsuitable because it induces side effects such as vasoconstriction and renal toxicity in mammals.[12-14] Therefore several approaches have been explored to overcome these challenges, including nanocarriers such as lipid vesicles[14] and biodegradable polymers.[12] The emerged focus on the encapsulation of Hb into nanosized carriers[15] is because nanoparticle-based erythrocyte mimics offer several distinct advantages, including 1) prevention of vasoconstriction, 2) avoidance of renal toxicity, and 3) the protection of Hb from degradation in bodily fluids to prolong the circulation time.[12]

Liposome-based carriers of Hb are one of the most important HBOC formulations and have been widely studied.[14-16] Liposome-encapsulated Hb with a size of 250 nm have been proved its safety and the elimination of vasoconstriction.[15, 17] However, plain liposomes are fragile and easily deform when exposed to fluid shear stresses.[14] Many strategies have been investigated to increase the liposome's mechanical strength, like using solid silica nanoparticle (diameter ~10 nm) as core for a rigid support,[7] introducing an actin matrix inside the aqueous core of submicron liposomes.[7, 14] Mesoporous silica nanoparticles (MSNs) can be used as protein delivery carriers due to their unique properties, namely biocompatibility, chemical inertness, large surface area and controllable pore size.[18-21] Inspired by nature, Brinker and others reported a versatile nanocarrier that synergistically integrates the advantages of liposomes with MSNs, resulting in lipid bilayer (LB) coated MSNs with a so-called "protocell" structure (Scheme 5.1).[18-20, 22-24] The electrostatic interaction of zwitterionic liposomes with the negatively charged MSNs surface, results in vesicle rupture and concomitant bilayer formation. As a result, the MSNs pores are sealed and entrapped the drug of interest inside the MSNs.[18, 19, 22, 25] Furthermore, the lipid bilayer act as an immune-isolative barrier, which can prevent recognition by the reticuloendothelial system and as a result enhance the circulation time.[26] Recently, nanosized-MSNs with large pore diameters (10 nm) and therefore capable of accommodating Hb inside have been developed in our group.

To increase the colloidal stability under physiological conditions and biocompatibility, a lipid bilayer was applied (LB-MSNs).[27] In addition, the charge-neutral highly hydrophilic polymer polyethylene glycol (PEG) was incorporated in the lipid bilayer to induce stealth-like behavior.[14, 28]

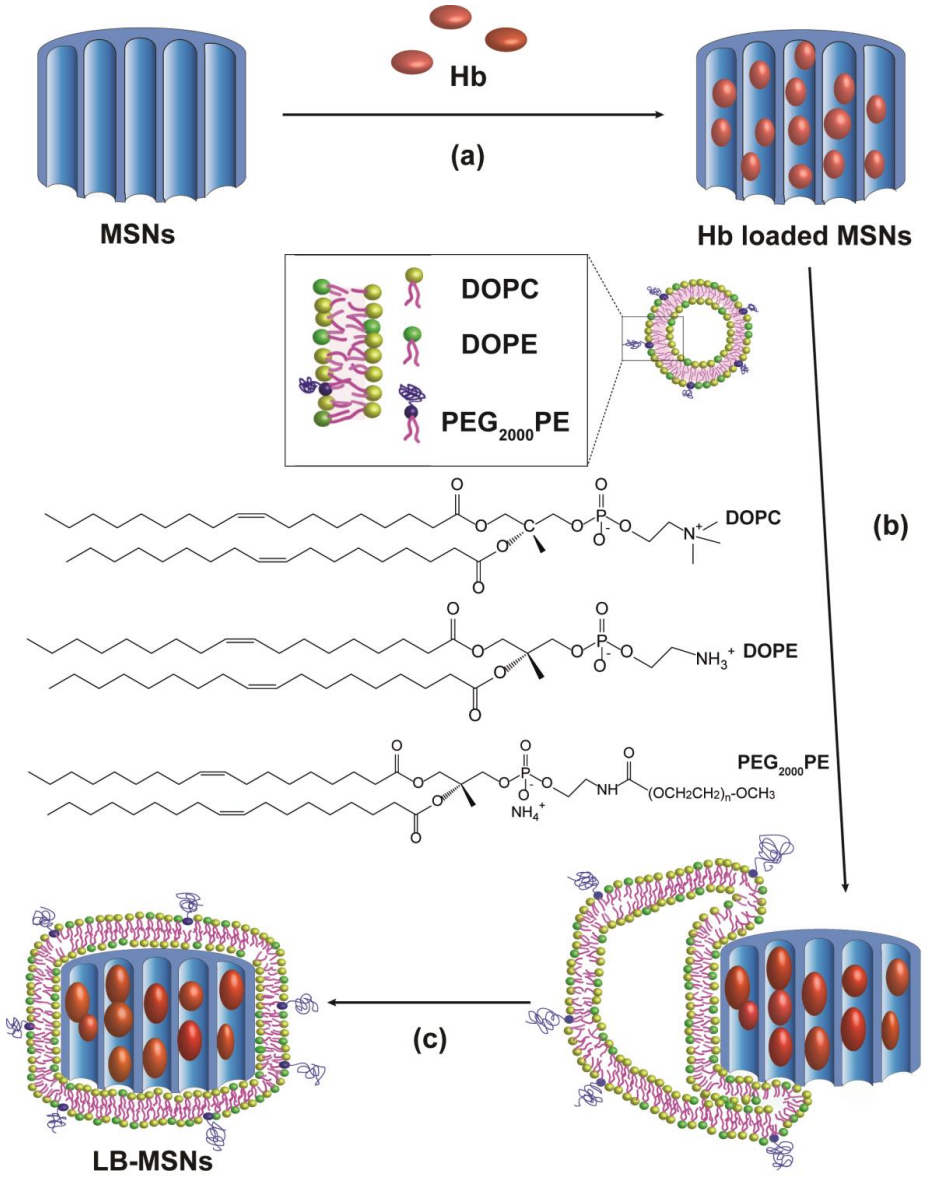

Scheme 5.1 *Procedure for the formation of LB-MSNs. (a) Encapsulation of Hb into the MSNs, followed by fusion of (b) liposome (composed of DOPC/DOPE/PEG$_{2000}$PE), resulting in (c) LB-MSNs (i.e. protocell).*

Herein, we demonstrate a facile method to prepare liposome encapsulated Hb-loaded MSNs (LB-MSNs) as a potential oxygen carrier. MSNs with a 10 nm channel diameter are used to accommodate Hb. To improve the colloidal stability of these Hb-loaded MSNs, a supported lipid bilayer was introduced to decorate the outer surface of Hb-loaded MSNs resulting in a core-shell structure. The preparation of these nanoparticles is schematically illustrated in Scheme 1. The presence of a lipid bilayer lowers the premature release of Hb. Circulation and distribution studies were performed in zebrafish embryos in order to investigate the *in vivo* behavior of the these lipid bilayer coated MSNs.

5.2 Experimental Section

5.2.1 Materials

Bovine hemoglobin (Hb, Mw~64500), Pluronic P123 ($EO_{20}PO_{70}EO_{20}$, M_n~5800), tetraethyl orthosilicate (TEOS, ≥98%), hydrochloric acid (HCl), 1,3,5-trimethylbenzene (TMB), 2',2'-azino-bis (3-ethylbenzothiazoline-6-sulfonic) acid (ABTS) and fluorescein isothiocyanate were purchased from Sigma-Aldrich and used as received. 1,2-dioleoyl-sn-glycero-3-phosphocholine (DOPC), 1,2-dioleoyl-sn-glycero-3-phosphoethanolamine (DOPE), 1,2-dioleoyl-sn-glycero-3-phosphoethanolamine-N-[methoxy(polyethylene glycol)-2000] (ammonium salt) ($PEG_{2000}PE$) and 1,2-dioleoyl-sn-glycero-3-phosphoethanolamine-N-(lissamine rhodamine B sulfonyl) (ammonium salt) (DOPE-LR) were purchased from Avanti Polar Lipids. Fluorocarbon surfactant FC-4 was purchased from Yick-Vic Chemicals & Pharmaceuticals (HK) Ltd. Sephadex G25 was purchased from GE Healthcare Life Sciences. The composition of the phosphate buffered saline (PBS) used was: K_2HPO_4 (14.99 mM), KH_2PO_4 (5 mM), and NaCl (150.07 mM), with an ionic strength of 270 mM. The phosphate buffer (PB) with an ionic strength of 12 mM was prepared by mixing Na_2HPO_4 (1 mM) and NaH_2PO_4 (1 mM) at molar ratio of 5:2. Milli-Q water (18.2 MΩ/cm, Millipore Co., USA) was used throughout the experiment. All Hb solutions for the experiments are freshly prepared before each experiment.

5.2.2 Synthesis of large-pore MSNs

MSNs were synthesized as follows. 0.5 g of surfactant Pluronic P123 and 1.4 g of FC-4 were dissolved in 80 mL of HCl (0.02 M), followed by the introduction of 0.48 mL of TMB. After stirring for 6 h, 2.14 mL of TEOS was added dropwise. The resulting mixture was stirred at 30 °C for 24 h and transferred to an autoclave at 120 °C for 2 days. Finally, the solid

product was isolated by centrifugation, and washed with ethanol and water. The organic template was completely removed by calcination at 550 °C for 5 h.

5.2.3 Preparation of liposome

Liposomes were prepared by dispensing stock solutions of DOPC (80 µl, 25 mg/mL), DOPE (40 µl, 25 mg/mL), and PEG_{2000}-PE (30 µl, 25 mg/mL) into scintillation vials. All lipids were dissolved in chloroform. A lipid film was formed by slow evaporation of chloroform in the vial under a nitrogen flow and kept under vacuum overnight. The lipid film was rehydrated by the addition of phosphate buffer (2 mL, 1 mM, pH 7.4) and the mixture was vortexed to form a cloudy lipid suspension. The obtained suspension was sonicated in a water bath (50 °C) for 10 min. If necessary, fluorescent lipids (DOPE-LR) were incorporated into the lipid mixture at 1 wt% to make fluorescent liposomes. The resulting liposomes were stored at 4 °C (final lipid concentration was 1.875 mg/mL).

5.2.4 Loading Hb into MSNs

MSNs were dispersed in phosphate buffer (PB, 1 mM, pH 7.4) at a concentration of 2 mg/mL and sonicated for 10 min. 0.5 mL of MSNs were mixed with a series of Hb with relatively low concentrations (0-700 µg/mL, 0.5 mL) and shaken using an Eppendorf mixer (400 rpm, 25 °C) for 10 min. Hb-loaded MSNs were collected by centrifugation (14000 rpm, 5 min) for further physical characterization and the amount of non-encapsulated Hb in the supernatant was quantified using a Tecan M1000 plate reader. A calibration curve was determined based on the absorbance at 405 nm as a function of Hb concentration (0-350 µg/mL).

The maximum loading capacity (LC%) of Hb in MSNs can be obtained by thermogravimetric analysis (TGA),[2] the same loading procedure was repeated by mixing MSNs suspensions and Hb with higher initial concentrations (0, 0.25, 0.5, 1, 1.5, 2, 3 and 4 mg/mL). Before thermogravimetric analysis (TGA), Hb-loaded MSNs were freeze-dried until the weight was constant. The loading capacity (LC%) was calculated according to equation 5.1:[29]

$$\text{LC } \% = \frac{\text{Loading}_{\text{Hb}}}{\text{Loading}_{\text{Hb}+\text{MSNs}}} \times 100\ \% \qquad (5.1)$$

Where $\text{Loading}_{\text{Hb}}$ represents the amount of Hb absorbed in the MSNs.

5.2.5 Preparation of LB-MSNs

To prepare LB-MSNs, 0.5 mL of Hb (0.5 mg/mL, PB) was transferred into a 2-mL Eppendorf tube, followed by the addition of a MSNs suspension (0.5 mL, 2 mg/mL). After shaking for 10 min, Hb-loaded MSNs were isolated by centrifugation. A dispersion (0.5 mL) of Hb-loaded MSNs (1 mg/mL) in PB (1 mM, pH 7.4) liposomes (composed of DOPC, DOPE, $PEG_{2000}PE$). The mixture was for 1.5 h (400 rpm, 25 °C). LB-MSNs were separated by centrifugation (13000 rpm, 5 min) from the excess of liposomes in the supernatant and then washed 3 times with PB. The hydrodynamic diameter and zeta-potential as a function of time were determined in 1 mM PB (pH 7.4) using a Malvern Nano-zs instrument. Hb-loaded MSNs (1:4 *w/w*) were used as control.

5.2.6 Characterization of MSNs, Hb-loaded MSNs and LB-MSNs

The morphology and mesostructure of the MSNs were characterized with scanning electron microscopy (SEM) and transmission electron microscopy (TEM). SEM imaging was conducted using a NovaSem microscope with an accelerating voltage of 15 kV and TEM imaging was conducted on a JEOL 1010 instrument with an accelerating voltage of 70 kV. Nitrogen adsorption-desorption isotherms were obtained with a Micromeritics TrisStar II 3020 surface area analyzer. Before the measurements, MSNs (at 300 °C) and Hb-loaded MSNs (at 25 °C) were outgassed in the instrument for 16 h under vacuum (< 0.15 mbar). The specific surface areas were calculated from the adsorption data in the low pressure range using the Brunauer-Emmett-Teller (BET) model.[30] The pore size distribution was determined following the Barrett-Joyner-Halenda (BJH) model.[31] The hydrodynamic size distribution and zeta-potential were measured with a Malvern Nano-zs instrument. Thermogravimetric analysis (TGA) was conducted with a Perkin Elmer TGA7. All the samples were tested under an air atmosphere from 25 °C to 800 °C at a heating rate of 10 °C/min. UV-Visible absorbance spectra were measured using 96-well plates with a Tecan M1000 plate reader. LB-MSNs were imaged by fluorescence microscopy (Zeiss Axio imager D2 fluorescence microscope, magnification 100×).

5.2.7 Peroxidase-like activity of Hb-loaded MSNs and Hb

The peroxidase-like activity of Hb after encapsulation by MSNs was measured using 2,2'-azino-bis(3-ethylbenzothiazoline-6-sulfonic acid) diammonium salt (ABTS).[6, 32]

An ABTS solution was prepared by dissolving 15 mg of ABTS in 1 mL MilliQ water and 9 mL acetic acid.[33] Hydrogen peroxide (1 mL, 30% *w/w* in water) was diluted into 30 mL of MilliQ water. Hb (0.05 and 0.1 mg/mL, 5 µl) and Hb-loaded MSNs (0.05 and 0.1 mg/mL, 5 µl) were mixed with hydrogen peroxide (150 µL) in 96-well plate followed by the immediate addition of the ABTS solution (45 µL). The absorbance at 418 nm of the oxidized blue-green $ABTS^{\cdot+}$ was monitored every 20 sec for 20 min using a plate reader (Tecan infinite M1000). The control experiment was performed by using enzyme-free PBS and plain MSNs (0.05 and 0.1 mg/mL) in PBS. All experiments were performed in triplicate.

5.2.8 Labeling of Hb with Fluorescein isothiocyanate

Hb (10 mg) was dissolved in 5 mL of sodium carbonate buffer (100 mM, pH 9). Fluorescein isothiocyanate (FITC) was dissolved in DMSO at 1 mg/mL, and 0.25 mL of the FITC solution was added to the protein solution. The mixture was stirred overnight at 4 °C. The resulting FITC-labelled Hb was purified by size exclusion chromatography using a Sephadex-G25 column and PBS as the eluent.

5.2.9 Release profiles of Hb from MSNs and LB-MSNs

The *in vitro* release profiles of Hb from MSNs and LB-MSNs were investigated by suspending Hb-loaded MSNs or LB-MSNs in PBS (warmed to 37 °C, pH 7.4) at a concentration of 1 mg/mL. The solution was incubated at 37 °C using an Eppendorf mixer (400 rpm). At various time points, the solution was centrifuged and the supernatants were replaced with fresh PBS. The released amount of Hb in the supernatant was determined with a Tecan M1000 plate reader. All analyses were performed in triplicate.

5.2.10 Zebrafish husbandry

Transgenic zebrafish of the Tg (kdrl:GFP) strain, which has a GFP reporter gene expressed specifically in the endothelial cells,[34-36] resulting in a green fluorescent vasculature. Zebrafish were handled in compliance with the local animal welfare regulations and maintained according to standard protocols (zfin.org). Embryos were raised in egg water (0.21 gm Instant Ocean sea salts in 1 liter of demi water) at 28.5 °C. For the duration of bacterial injections, embryos were kept under anesthesia in egg water containing 0.02% buffered 3-aminobenzoic acid ethyl ester (Tricaine). The

breeding of adult fish was approved by the local animal welfare committee (DEC) of the University of Leiden. All protocols adhered to the international guidelines specified by the EU Animal Protection Directive 2010/63/EU.

5.2.11 Zebrafish injection of LB-MSNs

A stock solution of LB-MSNs (5 mg/mL) and injected (5 μL) into the duct of cuvier. PBS injections were used as a control experiment. Injections were performed using a FemtoJet microinjector (Eppendorf) and a micromanipulator with pulled microcapillary pipettes.

5.2.12 Confocal microscopy imaging

Embryos were imaged after injection, embedded in 1% low melting point agarose and transferred to a Leica DMIRBE inverted microscope with a Leica SP1 confocal scan head for imaging with 40 or 63× lenses. For quantification purposes acquisition settings and area of imaging (in the caudal vein region) were kept the same across the groups.

5.3 Results and discussion

The morphology and mesoporous structure of the MSNs was analyzed by scanning electron microscopy (SEM) and transmission electron microscopy (TEM). From the SEM images, it became apparent that particles were non-spherical, the diameter of the as-prepared MSNs was found to be < 100 nm (Figure 5.1a). The TEM images more clearly visualized that the particles were 90 ± 20 nm long, with an average widths of 43 ± 7 nm (average of 150 nm particles). TEM imaging also revealed that the particles possessed an array of disc-shaped mesochannels that run parallel to the short axis of the MSNs (Figure 5.1b).

To characterize the channels within the cuboidal MSNs and to prove encapsulation of Hb molecules within the channels is possible, nitrogen sorption measurements were performed. Both MSNs and Hb-loaded MSNs, exhibited characteristic type IV isotherms with type H_1 hysteresis loops, showed that these nanoparticles have disc-like mesopores according to International Union of Pure and Applied Chemistry (IUPAC) classification.[37] The presence of encapsulated Hb does reduce the surface area from 506 m^2/g to 275 m^2/g. This is in agreement with the reduced average channel diameter from 10 nm (MSNs) to 7 nm (Hb-loaded MSNs), which was confirmed from the desorption branch of the isotherm using the Barrett-

Joyner-Halenda (BJH) method (Figure 5.1c,d). Upon Hb encapsulation, both surface area and pore diameter of the MSNs decreased, indicating that hemoglobin was indeed encapsulated within the channels of the MSNs.

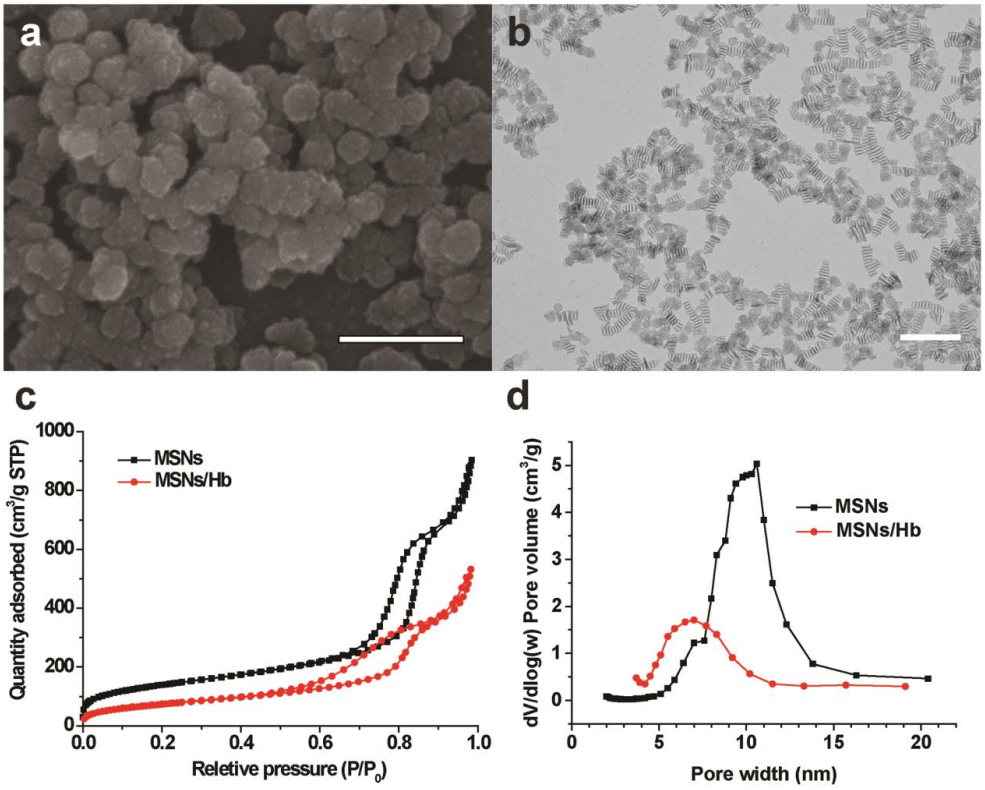

Figure 5.1 *(a and b) SEM and TEM images of MSNs. Scale bar = 250 nm. (c) Nitrogen adsorption-desorption isotherms and (d) plots of pore diameter vs. pore volume, calculated from the desorption isotherms using the BJH model, show that the MSNs and Hb loaded MSNs (146 mg/g) have an average pore diameter of 10 ± 1 nm and 7.5 ± 1.5 nm, respectively.*

Thermogravimetric analysis (TGA) is one of most commonly use methods to detect the drug loading effiency.[2, 37, 38] A half-life of cell-free Hb is relatively short (0.5-1.5 h), because of the dissociation of the Hb tetramer ($\alpha_2\beta_2$) into dimers ($2\alpha\beta$).[10] To reduce the errors, the percentage of Hb loaded within the MSNs was determined by TGA.[2] We observed that the weight loss upon heating the sample corresponding to the amount of Hb inside the MSNs for Hb correlated with the initial Hb concentration. Upon heating, both MSNs (as control) and MSNs/Hb (initial concentration, 4 mg/mL) underwent a total weight loss of 3.8% (H_1) and 42.1% (H_2) when measured up to

800 °C (Figure 5.2a). The initial weight loss up to 100 °C was caused by the removal of thermo-desorbed water corresponding to 1.5% (L_1) and 3.4% (L_2) of the total weight loss. The weight loss (W) corresponding to Hb was calculated according to the following equation 5.2:[39]

$$\frac{H1-L1}{100-H1} = \frac{H2-W-L2}{100-H2}$$

$$W = H_2 - L_2 - \frac{(H1-L1)(100-H2)}{100-H1} \quad (5.2)$$

L: the initial weight loss until 100 °C was caused by the presence of thermo-desorbed water; H: the total weight loss up to 800 °C; Plain MSNs were used as control, L_1 (100 °C) and H_1 (800 °C).

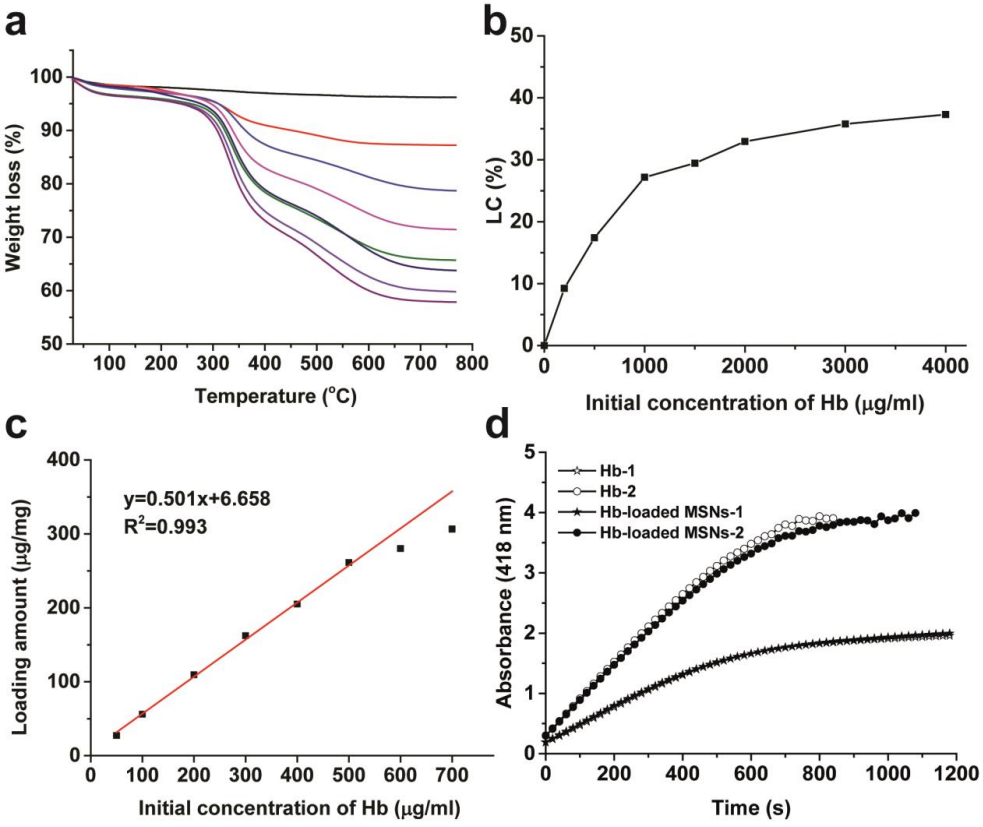

Figure 5.2 *(a) TGA curves of Hb-loaded MSNs with different initial concentrations of Hb (0, 0.25, 0.5, 1, 1.5, 2, 3 and 4 mg/mL, from top to bottom) and its corresponding b) LC% of Hb into MSNs calculated by TGA; (c) Loading amount of Hb into MSNs at low loading concentrations by a Tecan M1000 plate reader, absorbance at 405 nm, 0-700 μg/mL); (d)*

ABTS catalyzed by native Hb (white) and MSNs/Hb (black). Hb-1 and Hb-loaded MSNs-1 represent the initial concentration of Hb were 50 μg/mL and Hb-2 and Hb-loaded MSNs-2 were 100 μg/mL. The enzymatic activity of Hb was measured at 418 nm by examining the catalytic conversion of the oxidation of ABTS.

When the initial concentration of Hb used to load the MSNs was 4 mg/mL, the maximum loading capacity (37.3%) was obtained (Figure 5.2b). To investigate the encapsulation procedure in more detail, MSNs (2 mg/mL) were loaded with Hb using concentration range of this protein (0-700 μg/mL). This revealed that Hb loading in MSNs is a linearly correlated (R^2 = 0.993) with the initial Hb concentration (0-700 μg/mL, Figure 5.2c). At higher initial concentration of Hb this correlation is lost, because concentrated Hb competing for the encapsulation, leading the blockage of pores (Figure 5.2b,c).

Hemoglobin can act as a peroxidase-like protein as its heme center catalyses the reduction of hydrogen peroxide. Compared to inorganic catalysts, proteins (Hb) have a high substrate specificity and reactive efficiency under normal conditions.[6] To examine the enzymatic activity of encapsulated Hb, the oxidation of ABTS by hydrogen peroxide was used as an indicator.[6] The catalytic reactivity of MSNs/Hb was analyzed and compared with native Hb in solution (Hb concentrations, 0.025 and 0.5 mg/mL). As shown in Figure 5.3b,c, the kinetics of the two enzyme-catalyzed reactions are essentially identical, indicating that the encapsulated Hb in MSNs exhibit high peroxidase-like activity as native Hb in aqueous solution.[32] As expected, a higher concentration of Hb resulting a faster conversion of H_2O_2. This result indicated that after encapsulation, Hb remained its peroxidase-like activity of Hb was not altered.

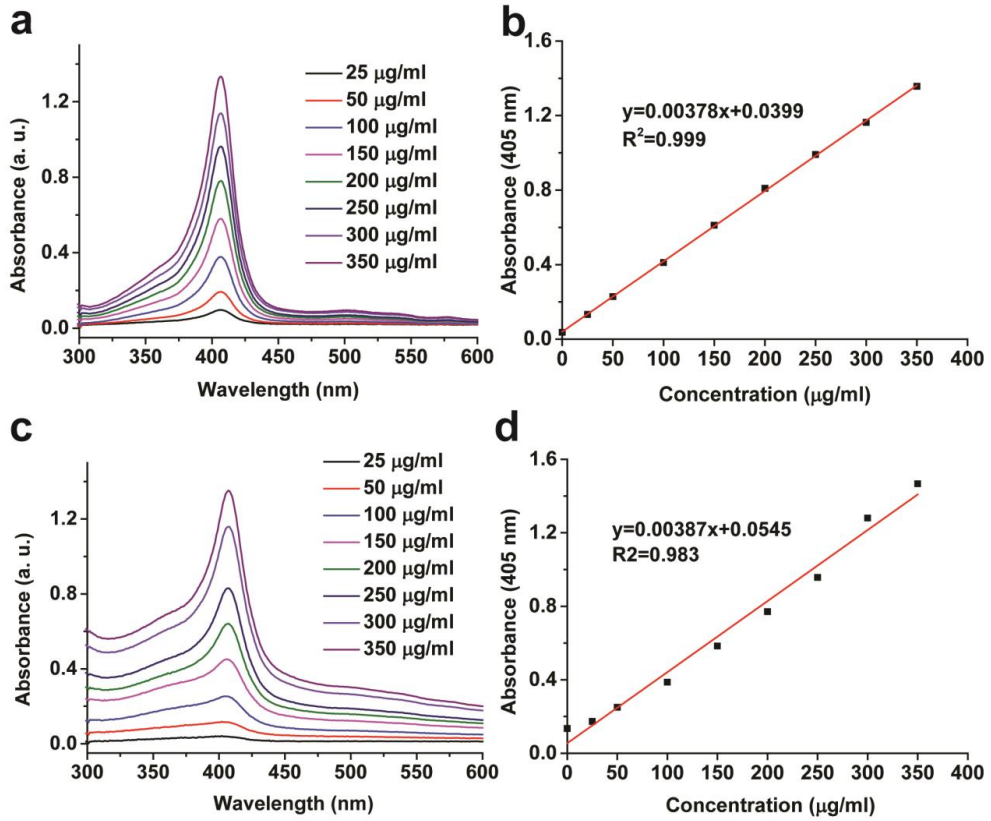

Figure 5.3 *(a) UV-VIS absorption spectra of Hb at varying concentrations (25-350 μg/mL); (b) standard curve of Hb absorbance (405 nm); (c) UV-Visible absorption spectra of Hb-loaded MSNs with varying concentration (based on Hb, 25-350 μg/mL); (d) standard curve of Hb-loaded MSNs (405 nm).*

Helpful information on the heme protein folding can be obtained. From the Soret band in the UV-Visible absorption spectrum of hemoglobin as it is sensitive to the microenvironment, substructure, and oxidation state.[40] The spectral characteristics of MSNs/Hb (Hb concentration: 25-350 μg/mL) showed absorption curves that the closely resembled those of native Hb as in all cases the maximum absorption was centered at 405 nm and no blue-shift was observed, suggesting no occurrence of protein unfolding.[41] The only noticeable difference is that MSNs/Hb showed some slight peak broadening, probably caused by the light scattering of MSNs (Figure 5.3a,c). A good linear relationship (R^2 = 0.983) between the absorbance (405 nm) and MSNs/Hb concentration was obtained, similar to native Hb (Figure 5.3b,d, R^2 = 0.999).

This confirms that Hb retains its higher-order structure in the mesopores of MSNs and does not undergo significant denaturation after encapsulation inside the silica pores.[6, 40]

Efficient encapsulation of Hb into MSNs occurs when the physicochemical properties of the Hb surface and the MSNs are complementary.[42] As the isoelectric point (pI) of Hb is 6.8-7.0 and 2-3 for the MSNs.[15, 42] both MSNs and Hb are negatively charged at physiological pH (7.4). The amount of Hb encapsulated in the MSNs was dependent on its initial concentration, indicating that the adsorption process was probably driven by capillary action.[43] Hb was encapsulated into the mesoporous channels (Figure 5.1c,d), but also the encapsulation process on the outer surface of the MSNs (Figure 5.S1). At higher Hb concentrations, the hydrodynamic diameter of Hb-loaded MSNs increased dramatically due to aggregation (Figure 5.S1a). Therefore a lipid bilayer was introduced to coat the Hb-loaded MSNs and form a physical barrier preventing colloidal aggregation (Figure 5.4a). The long-term colloidal stability of LB-MSNs is an important criteria for future biomedical applications. The hydrodynamic diameter and the zeta-potential of LB-MSNs were therefore measured for one week. The hydrodynamic diameter and the zeta-potential remained stable within this period (~250 nm, ~-23 mV) for at least one week (Figure 5.4b,c). Next, the cumulative release of Hb from MSNs and LB-MSNs was studied *in vitro* (Figure 5.4d). Hb-loaded MSNs (1:4 *w/w*) showed a burst release during the first hour with a release amount of 25.50 ± 0.33%, while for LB-MSNs this was decreased to 6.73 ± 0.83%. After 180 h, the cumulative release percentage of Hb-loaded MSNs and LB-MSNs was 42.27 ± 0.60% and 27.49 ± 0.29%, respectively. This shows that the lipid bilayer physically lowers the amount of Hb leaching out from the MSNs (Figure 5.4d).

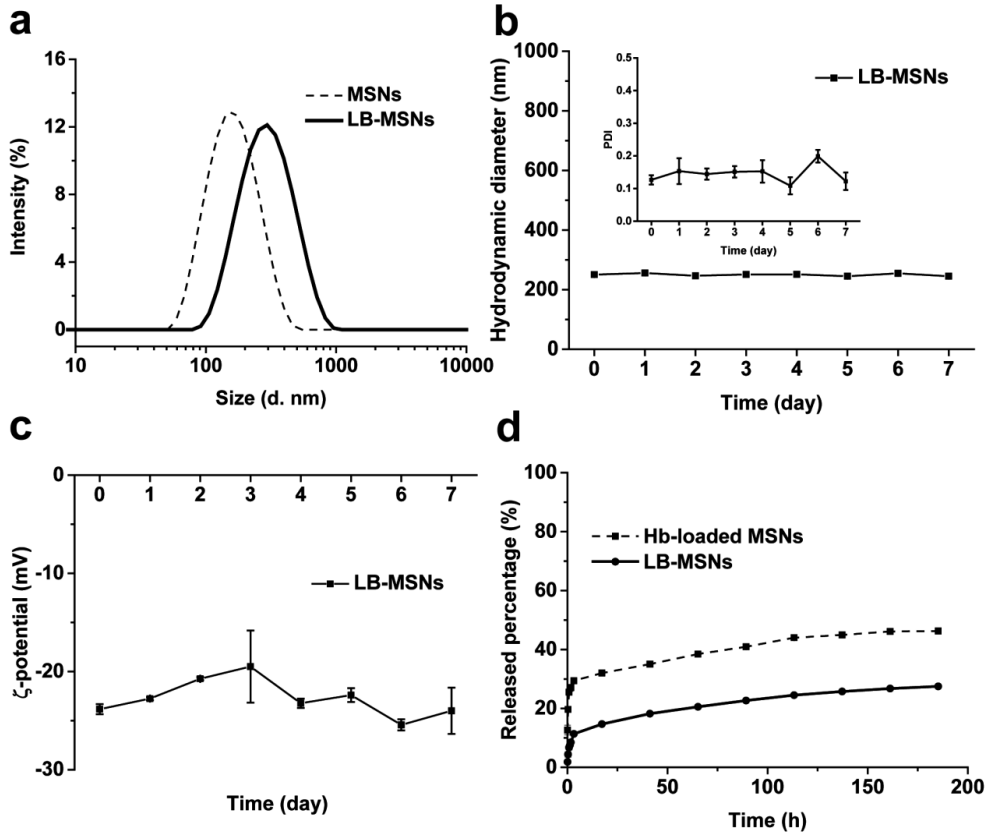

Figure 5.4 *Colloidal stability of LB-MSNs. (a) Hydrodynamic diameter of MSNs and LB-MSNs according to DLS (1 mM PB, pH 7.4); (b) size stability (insert: PDI values) and (c) zeta-potential of LB-MSNs were measured as a function of time (1 mM PB, pH 7.4); (d) release profiles of Hb-loaded MSNs and LB-MSNs in PBS (37 °C, pH 7.4).*

Fluorescence microscopy imaging was used to visualize and confirm the localization of Hb within the nanoparticles using fluorescent microscopy. For this, Hb was labelled with fluorescein isothiocyanate (FITC) while DOPE-LR was used to visualize the lipid bilayer on the Hb-loaded MSNs (Figure 5.S2). Due to the low magnification (100×) of the microscope and the small particle size (~250 nm, Figure 5.4a,b), it was not possible to observe single particle with great detail. Still the overlap of both dyes is a clear indication of the co-localization of Hb and the lipid bilayer at the same particle. Furthermore, the uniform distribution of LB-MSNs on the silicon slide proved the LB-MSNs were well-dispersed.

Zebrafish (*Danio rerio*) embryos have emerged as an important transparent vertebrate model and are useful *in vivo* model for real-time imaging technique of a wide activity of biological processes and to study the distribution and circulation of nanoparticles.[34, 44, 45] To study the *in vivo* behaviour of Hb loaded LB-MSNs in circulation, we injected fluorescent labelled LB-MSNs into the blood circulation system. After injection, the nanoparticles moved with the blood flow and readily distributed throughout the circulation of the bloodstream as evidenced by confocal imaging[35] (Figure 5).

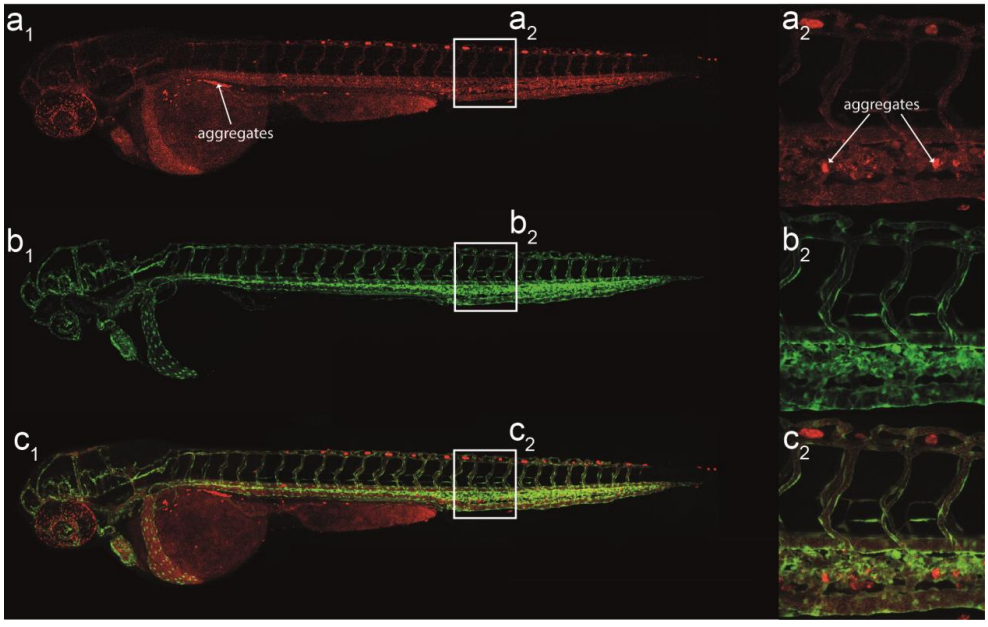

Figure 5.5 *Confocal fluorescence images of (a) lissamine rhodamine labeled LB-MSNs), with a few regular red dots attributed to autofluorescence, (b) GFP expressed blood vessels of a zebrafish embryo, (c) overlay images show the localization of the LB-MSNs in the blood vessels.*

Imaging revealed that LB-MSNs could systemic circulate and are evenly distributed in the blood vessels, with only little aggregation in the caudal hematopoietic tissue and the dorsal region of the yolk sac (Figure 5.5). The large majority of the nanoparticles however did not interact with endothelium, only a few adhered to the endothelium lining of the blood vessel and were trapped as expected. PEGylation of nanoparticle has shown to be an effective method to lower the binding affinity of the

particles for endothelial cells *in vivo*.[35] However, further optimization of the lipid bilayer composition and the amount of PEGylation are planned.

5.4 Conclusion

In summary, lipid bilayer coated MSNs were used as a carrier for Hb. The large disc-like pores of the MSNs enabled the rapid encapsulation of Hb into the mesopores with a high loading capacity. Encapsulated Hb remained active and exhibited similar enzymatic activity to non-encapsulated Hb. The introduction of a supported lipid bilayer prevented premature Hb release from LB-MSNs and improved the colloidal stability *in vitro*. These Hb loaded LB-MSNs could be considered as an artificial erythrocyte mimic. Only the circulation and distribution of the LB-MSNs was tested in zebrafish embryos. Unfortunately, convective blood flow is not essential to supply oxygen to the tissues during the early larval development of zebrafish.[46] Therefore Hb oxygen transport had no effect on oxygen-dependent processes[47] as even mutant zebrafish lacking erythrocytes survive for about 2 weeks after fertilization.[46, 48] Further testing using other animal models (*e.g.* mice) are therefore required to test these Hb-loaded MSNs as a mimic for red-blood cells.

Supporting information

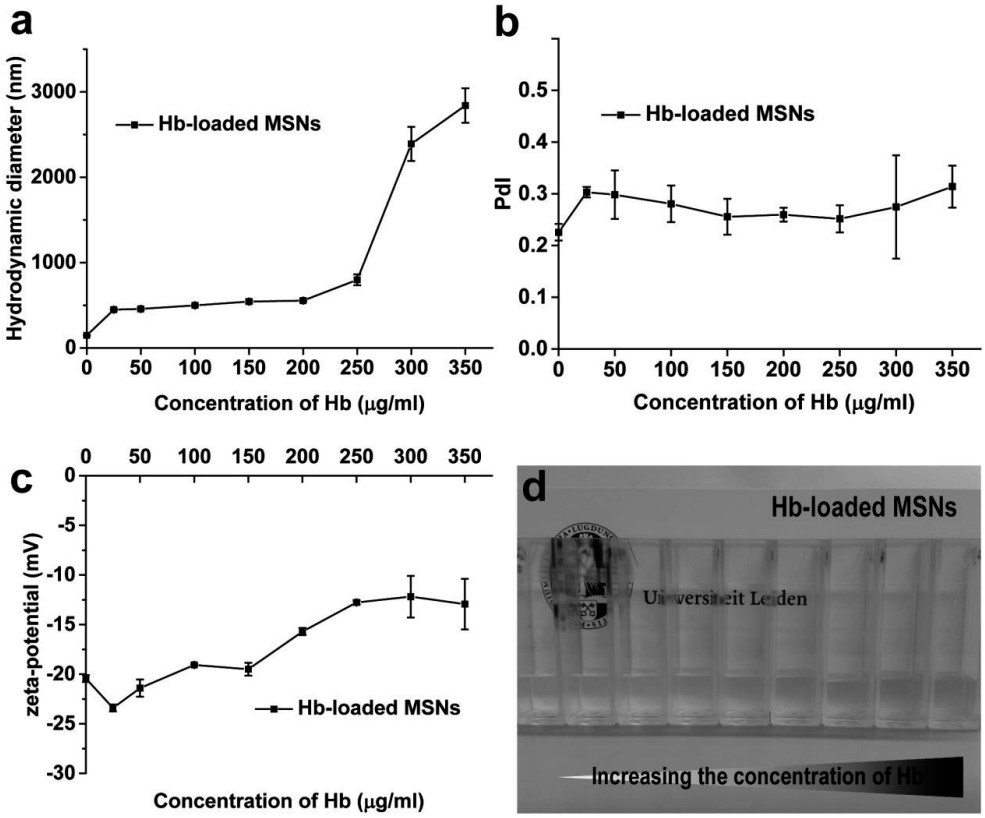

Figure 5.S1 *(a) Hydrodynamic diameter of Hb-loaded MSNs with varying concentrations (0-350 μg/mL) and the corresponding (b) PDI values, (c) zeta-potential in 1 mM PB (pH 7.4); (d) digital photograph of Hb-loaded MSNs with increasing concentration of Hb from the left to the right.*

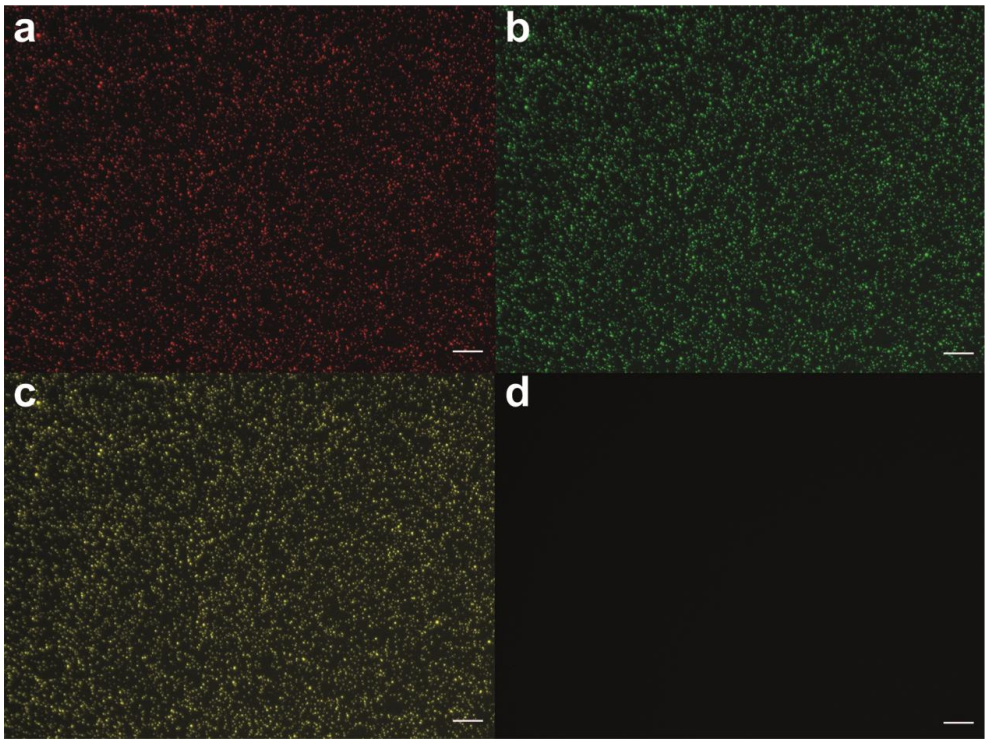

Figure 5.S2 *(a) Fluorescence images of LB-MSNs on silicon slides, the scale bar represents 100 µm. (a) liposomes labelled with 1wt% DOPE-LR, (excitation wavelength = 546 nm); (b) FITC-labelled Hb (excitation wavelength = 488 nm); (c) overlay image, (d) control, empty silicon slide (magnification 100×).*

5.5 References

1. W. Q. Wang, S. Liu, Y. B. Huang, X. B. Jing and Z. G. Xie, *J. Mater. Chem. B*, 2015, 3, 5753-5759.
2. L. Duan, X. H. Yan, A. H. Wang, Y. Jia and J. B. Li, *ACS Nano*, 2012, 6, 6897-6904.
3. H. G. Klein, D. R. Spahn and J. L. Carson, *Lancet*, 2007, 370, 415-426.
4. T. Henkel-Honke and M. Oleck, *AANA J.*, 2007, 75, 205-211.
5. D. R. Spahn, *Crit. Care*, 1999, 3, R93-R97.
6. Y. Urabe, T. Shiomi, T. Itoh, A. Kawai, T. Tsunoda, F. Mizukami and K. Sakaguchi, *Chembiochem*, 2007, 8, 668-674.
7. M. X. Liu, L. H. Gan, L. H. Chen, D. Z. Zhu, Z. J. Xu, Z. X. Hao and L. W. Chen, *Int. J. Pharm.*, 2012, 427, 354-357.
8. K. Chen, T. J. Merkel, A. Pandya, M. E. Napier, J. C. Luft, W. Daniel, S. Sheiko and J. M. DeSimone, *Biomacromolecules*, 2012, 13, 2748-2759.
9. T. M. S. Chang, *Artif. Cells, Blood Substitutes, Biotechnol.*, 2012, 40, 197-199.
10. E. Tsuchida, K. Sou, A. Nakagawa, H. Sakai, T. Komatsu and K. Kobayashi, *Bioconjugate Chem.*, 2009, 20, 1419-1440.
11. T. M. S. Chang, *Artif. Organs*, 2004, 28, 789-794.
12. J. Zhao, C. S. Liu, Y. Yuan, X. Y. Tao, X. Q. Shan, Y. Sheng and F. Wu, *Biomaterials*, 2007, 28, 1414-1422.
13. Y. Xiong, A. Steffen, K. Andreas, S. Muller, N. Sternberg, R. Georgieva and H. Baumler, *Biomacromolecules*, 2012, 13, 3292-3300.
14. S. L. Li, J. Nickels and A. F. Palmer, *Biomaterials*, 2005, 26, 3759-3769.
15. W. Gao, B. Y. Sha, W. Zou, X. Liang, X. Z. Meng, H. Xu, J. Tang, D. C. Wu, L. X. Xu and H. Zhang, *Biomaterials*, 2011, 32, 9425-9433.
16. H. Sakai, K. Tomiyama, K. Sou, S. Takeoka and E. Tsuchida, *Bioconjugate Chem.*, 2000, 11, 425-432.
17. H. Sakai, H. Horinouchi, Y. Masada, S. Takeoka, E. Ikeda, M. Takaori, K. Kobayashi and E. Tsuchida, *Biomaterials*, 2004, 25, 4317-4325.
18. J. Liu, X. Jiang, C. Ashley and C. J. Brinker, *J. Am. Chem. Soc.*, 2009, 131, 7567-7569.
19. J. W. Liu, A. Stace-Naughton, X. M. Jiang and C. J. Brinker, *J. Am. Chem. Soc.*, 2009, 131, 1354-1355.
20. J. W. Liu, A. Stace-Naughton and C. J. Brinker, *Chem. Commun.*, 2009, 5100-5102.
21. I. I. Slowing, C. W. Wu, J. L. Vivero-Escoto and V. S. Y. Lin, *Small*, 2009, 5, 57-62.
22. H. Meng, M. Wang, H. Liu, X. Liu, A. Situ, B. Wu, Z. Ji, C. H. Chang and A. E. Nel, *ACS Nano*, 2015, 3540–3557.
23. C. E. Ashley, E. C. Carnes, G. K. Phillips, D. Padilla, P. N. Durfee, P. A. Brown, T. N. Hanna, J. Liu, B. Phillips, M. B. Carter, N. J. Carroll, X. Jiang, D. R. Dunphy, C. L. Willman, D. N. Petsev, D. G. Evans, A. N. Parikh, B. Chackerian, W. Wharton, D. S. Peabody and C. J. Brinker, *Nat. Mater.*, 2011, 10, 389-397.
24. P. N. Durfee, Y. S. Lin, D. R. Dunphy, A. J. Muniz, K. S. Butler, K. R. Humphrey, A. J. Lokke, J. O. Agola, S. S. Chou, I. M. Chen, W. Wharton, J. L. Townson, C. L. Willman and C. J. Brinker, *ACS Nano*, 2016, 8325-8345.
25. S. Mornet, O. Lambert, E. Duguet and A. Brisson, *Nano Lett.*, 2005, 5, 281-285.
26. D. R. Arifin and A. F. Palmer, *Biotechnol. Prog.*, 2003, 19, 1798-1811.
27. M. Bouchoucha, R. C-Gaudreault, M. A. Fortin and F. Kleitz, *Adv. Funct. Mater.*, 2014, 24, 5911-5923.
28. G. Y. Tonga, K. Saha and V. M. Rotello, *Adv. Mater.*, 2014, 26, 359-370.

29. X. X. Zhang, F. F. Li, S. Y. Guo, X. Chen, X. L. Wang, J. Li and Y. Gan, *Biomaterials*, 2014, 35, 3650-3665.
30. E. P. H. Brunauer S. , Teller E., *J. Am. Chem. Soc.*, 1938, 60, 309-319.
31. E. P. Barrett, L. G. Joyner and P. P. Halenda, *J. Am. Chem. Soc.*, 1951, 73, 373-380.
32. I. I. Slowing, B. G. Trewyn and V. S. Y. Lin, *J. Am. Chem. Soc.*, 2007, 129, 8845-8849.
33. M. Takayanagi and T. Yashiro, *Clin. Chem.*, 1984, 30, 357-359.
34. L. Evensen, P. L. Johansen, G. Koster, K. Zhu, L. Herfindal, M. Speth, F. Fenaroli, J. Hildahl, S. Bagherifam, C. Tulotta, L. Prasmickaite, G. M. Maelandsmo, E. Snaar-Jagalska and G. Griffiths, *Nanoscale*, 2016, 8, 862-877.
35. P. L. Johansen, F. Fenaroli, L. Evensen, G. Griffiths and G. Koster, *Nat. Commun.*, 2016, 7.
36. J. Choi, L. Dong, J. Ahn, D. Dao, M. Hammerschmidt and J. N. Chen, *Dev. Biol.*, 2007, 304, 735-744.
37. B. L. Zhang, Z. Luo, J. J. Liu, X. W. Ding, J. H. Li and K. Y. Cai, *J. Controlled Release*, 2014, 192, 192-201.
38. Y. Zhang, Z. Zhi, T. Jiang, J. Zhang, Z. Wang and S. Wang, *J. Controlled Release*, 2010, 145, 257-263.
39. M. Xie, H. Shi, Z. Li, H. J. Shen, K. Ma, B. Li, S. Shen and Y. Jin, *Colloids Surf., B*, 2013, 110, 138-147.
40. Y. Xian, Y. Xian, L. Zhou, F. Wu, Y. Ling and L. Jin, *Electrochem. Commun.*, 2007, 9, 142-148.
41. J. Wu, X. Li, Y. Yan, Y. Hu, Y. Zhang and Y. Tang, *J. Colloid Interface Sci.*, 2013, 406, 130-138.
42. S. Hudson, J. Cooney and E. Magner, *Angew. Chem., Int. Ed.*, 2008, 47, 8582-8594.
43. X. Liu, L. Zhu, T. Zhao, J. Lan, W. Yan and H. Zhang, *Microporous Mesoporous Mater.*, 2011, 142, 614-620.
44. F. Sharif, F. Porta, A. H. Meijer, A. Kros and M. K. Richardson, *Int. J. Nanomed.*, 2012, 7, 1875-1890.
45. R. M. White, A. Sessa, C. Burke, T. Bowman, J. LeBlanc, C. Ceol, C. Bourque, M. Dovey, W. Goessling, C. E. Burns and L. I. Zon, *Cell Stem Cell*, 2008, 2, 183-189.
46. S. Grillitsch, N. Medgyesy, T. Schwerte and B. Pelster, *J. Exp. Biol.*, 2005, 208, 309-316.
47. B. Pelster and W. W. Burggren, *Circ. Res.*, 1996, 79, 358-362.
48. B. M. Weinstein, A. F. Schier, S. Abdelilah, J. Malicki, L. SolnicaKrezel, D. L. Stemple, D. Y. R. Stainier, F. Zwartkruis, W. Driever and M. C. Fishman, *Development*, 1996, 123, 303-309.
49. J. Tamayo, *Nat. Nanotechnol.*, 2015, 10, 738-739.
50. T. E. Angel, U. K. Aryal, S. M. Hengel, E. S. Baker, R. T. Kelly, E. W. Robinson and R. D. Smith, *Chem. Soc. Rev.*, 2012, 41, 3912-3928.
51. J. Shang and X. H. Gao, *Chem. Soc. Rev.*, 2014, 43, 7267-7278.
52. R. P. Carney, J. Y. Kim, H. F. Qian, R. C. Jin, H. Mehenni, F. Stellacci and O. M. Bakr, *Nat. Commun.*, 2011, 2.
53. S. Bruckenstein and M. Shay, *Electrochim. Acta*, 1985, 30, 1295-1300.
54. D. A. Buttry and M. D. Ward, *Chem. Rev.*, 1992, 92, 1355-1379.
55. M. Rodahl, F. Hook, A. Krozer, P. Brzezinski and B. Kasemo, *Rev. Sci. Instrum.*, 1995, 66, 3924-3930.
56. A. Janshoff, H. J. Galla and C. Steinem, *Angew. Chem., Int. Ed.*, 2000, 39, 4004-4032.
57. T. P. Burg, M. Godin, S. M. Knudsen, W. Shen, G. Carlson, J. S. Foster, K. Babcock and S. R. Manalis, *Nature*, 2007, 446, 1066-1069.

58. M. Fakruddin, Z. Hossain and H. Afroz, *J. Nanobiotechnol.*, 2012, 10.
59. J. Chaste, A. Eichler, J. Moser, G. Ceballos, R. Rurali and A. Bachtold, *Nat. Nanotechnol.*, 2012, 7, 300-303.
60. M. S. Hanay, S. Kelber, A. K. Naik, D. Chi, S. Hentz, E. C. Bullard, E. Colinet, L. Duraffourg and M. L. Roukes, *Nat. Nanotechnol.*, 2012, 7, 602-608.
61. M. Godin, A. K. Bryan, T. P. Burg, K. Babcock and S. R. Manalis, *Appl. Phys. Lett.*, 2007, 91.
62. W. H. Grover, A. K. Bryan, M. Diez-Silva, S. Suresh, J. M. Higgins and S. R. Manalis, *Proc. Natl. Acad. Sci. U. S. A.*, 2011, 108, 10992-10996.
63. Y. T. Yang, C. Callegari, X. L. Feng, K. L. Ekinci and M. L. Roukes, *Nano Lett.*, 2006, 6, 583-586.
64. A. Malloy, *Mater. Today*, 2011, 14, 170-173.
65. V. Filipe, A. Hawe and W. Jiskoot, *Pharm. Res.*, 2010, 27, 796-810.
66. T. Ito, L. Sun, M. A. Bevan and R. M. Crooks, *Langmuir*, 2004, 20, 6940-6945.
67. Z. Gu, A. Biswas, M. Zhao and Y. Tang, *Chem. Soc. Rev.*, 2011, 40, 3638-3655.
68. F. P. Chang, Y. P. Chen and C. Y. Mou, *Small*, 2014, 10, 4785-4795.
69. Z. Gao and I. Zharov, *Chem. Mater.*, 2014, 26, 2030-2037.
70. C.-H. Lee, T.-S. Lin and C.-Y. Mou, *Nano Today*, 2009, 4, 165-179.
71. J. Sun, H. Zhang, R. Tian, D. Ma, X. Bao, D. S. Su and H. Zou, *Chem. Comm.*, 2006, 1322-1324.
72. D. Y. Zhao, J. L. Feng, Q. S. Huo, N. Melosh, G. H. Fredrickson, B. F. Chmelka and G. D. Stucky, *Science*, 1998, 279, 548-552.
73. J. Gu, K. Huang, X. Zhu, Y. Li, J. Wei, W. Zhao, C. Liu and J. Shi, *J. Colloid Interface Sci.*, 2013, 407, 236-242.
74. N. Z. Knezevic and J. O. Durand, *Nanoscale*, 2015, 7, 2199-2209.
75. H. K. Na, M. H. Kim, K. Park, S. R. Ryoo, K. E. Lee, H. Jeon, R. Ryoo, C. Hyeon and D. H. Min, *Small*, 2012, 8, 1752-1761.
76. X. Du, L. Xiong, S. Dai, F. Kleitz and S. Z. Qiao, *Adv. Funct. Mater.*, 2014, 24, 7627-7637.
77. S. B. Hartono, N. T. Phuoc, M. H. Yu, Z. F. Jia, M. J. Monteiro, S. H. Qiao and C. Z. Yu, *J. Mater. Chem. B*, 2014, 2, 718-726.
78. M. Y. Wu, Q. S. Meng, Y. Chen, Y. Y. Du, L. X. Zhang, Y. P. Li, L. L. Zhang and J. L. Shi, *Adv. Mater.*, 2015, 27, 215-222.
79. F. Gao, P. Botella, A. Corma, J. Blesa and L. Dong, *J. Phys. Chem. B*, 2009, 113, 1796-1804.
80. Y. Han and J. Y. Ying, *Angew. Chem., Int. Ed.*, 2005, 44, 288-292.
81. H. Zhang, J. M. Sun, D. Ma, X. H. Bao, A. Klein-Hoffmann, G. Weinberg, D. S. Su and R. Schlogl, *J. Am. Chem. Soc.*, 2004, 126, 7440-7441.
82. J. Fan, J. Lei, L. Wang, C. Yu, B. Tu and D. Zhao, *Chem. Comm.*, 2003, 2140-2141.
83. M. Zaric, O. Lyubomska, O. Touzelet, C. Poux, S. Al-Zahrani, F. Fay, L. Wallace, D. Terhorst, B. Malissen, S. Henri, U. F. Power, C. J. Scott, R. F. Donnelly and A. Kissenpfennig, *ACS Nano*, 2013, 7, 2042-2055.
84. S. A. Coulman, A. Anstey, C. Gateley, A. Morrissey, P. McLoughlin, C. Allender and J. C. Birchall, *Int. J. Pharm.*, 2009, 366, 190-200.
85. P. C. DeMuth, X. F. Su, R. E. Samuel, P. T. Hammond and D. J. Irvine, *Adv. Mater.*, 2010, 22, 4851-4856.
86. K. van der Maaden, W. Jiskoot and J. Bouwstra, *J. Controlled Release*, 2012, 161, 645-655.
87. S. S. Wang, F. Yuan, K. Chen, G. J. Chen, K. H. Tu, H. J. Wang and L. Q. Wang, *Biomacromolecules*, 2015, 16, 2693-2700.

88. Y. Wang, Y. A. Nor, H. Song, Y. N. Yang, C. Xu, M. H. Yu and C. Z. Yu, *J. Mater. Chem. B*, 2016, 4, 2646-2653.
89. K. Lee, E. A. Silva and D. J. Mooney, *J. R. Soc., Interface*, 2011, 8, 153-170.
90. M. Cross and T. M. Dexter, *Cell*, 1991, 64, 271-280.
91. T. P. Richardson, M. C. Peters, A. B. Ennett and D. J. Mooney, *Nat. Biotechnol.*, 2001, 19, 1029-1034.
92. F. M. Chen, M. Zhang and Z. F. Wu, *Biomaterials*, 2010, 31, 6279-6308.
93. K. Y. Lee and S. H. Yuk, *Prog. Polym. Sci.*, 2007, 32, 669-697.
94. B. Chatin, M. Mevel, J. Devalliere, L. Dallet, T. Haudebourg, P. Peuziat, T. Colombani, M. Berchel, O. Lambert, A. Edelman and B. Pitard, *Mol. Ther.--Nucleic Acids*, 2015, 4, e244.
95. T. D. Dziubla, V. V. Shuvaev, N. K. Hong, B. J. Hawkins, M. Madesh, H. Takano, E. Simone, M. T. Nakada, A. Fisher, S. M. Albelda and V. R. Muzykantov, *Biomaterials*, 2008, 29, 215-227.
96. L. Schoonen and J. C. M. van Hest, *Adv. Mater.*, 2015, 1109-1128.
97. V. Nadithe and Y. H. Bae, *Tissue Eng., Part A*, 2011, 17, 2453-2462.
98. X. Li, Y. J. Chen, M. Q. Wang, Y. J. Ma, W. L. Xia and H. C. Gu, *Biomaterials*, 2013, 34, 1391-1401.
99. A. Fire, S. Q. Xu, M. K. Montgomery, S. A. Kostas, S. E. Driver and C. C. Mello, *Nature*, 1998, 391, 806-811.
100. J. Conde, A. Ambrosone, Y. Hernandez, F. Tian, M. McCully, C. C. Berry, P. V. Baptista, C. Tortiglione and J. M. de la Fuente, *Nano Today*, 2015, 10, 421-450.
101. X. Xu, J. Wu, Y. Liu, M. Yu, L. Zhao, X. Zhu, S. Bhasin, Q. Li, E. Ha, J. Shi and O. C. Farokhzad, *Angew. Chem., Int. Ed.*, 2016, 55, 7091-7094.
102. C.-f. Xu and J. Wang, *Asian J. Pharm. Sci.*, 2015, 10, 1-12.
103. Y. Jiang, R. Tang, B. Duncan, Z. Jiang, B. Yan, R. Mout and V. M. Rotello, *Angew. Chem., Int. Ed.*, 2015, 54, 506-510.
104. J. Tu, T. Wang, W. Shi, G. Wu, X. Tian, Y. Wang, D. Ge and L. Ren, *Biomaterials*, 2012, 33, 7903-7914.